Materials Research Bulletin 106 (2018) 228–233

Contents lists available at ScienceDirect

Materials Research Bulletin

journal homepage: www.elsevier.com/locate/matresbu

Optimization of crystal growth and properties of γ-CuI ultrafast scintillator by the addition of LiI

Shuangqiang Yue[a], Mu Gu[a,*], Xiaolin Liu[a], Fengrui Li[a], Shenye Liu[b], Xing Zhang[b], Juannan Zhang[a], Bo Liu[a], Shiming Huang[a], Chen Ni[a]

[a] Shanghai Key Laboratory of Special Artificial Microstructure Material & Technology, School of Physics Science and Engineering, Tongji University, Shanghai 200092, PR China

[b] Research Centre of Laser Fusion, Chinese Academy of Engineering Physics, Mianyang, 621900, PR China

ARTICLE INFO

Keywords:
γ-CuI crystal growth
Evaporation technique
LiI doping
Luminescence

ABSTRACT

Large-sized γ-CuI single crystals with ultrafast scintillation property were grown in LiI acetonitrile solvent through evaporation technique. The LiI exhibits unique properties to γ-CuI single crystal preparation. One is that it increases the solubility of CuI in the solvent, which gives rise to a largest-sized (23 × 14 × 2 mm^3) single crystal with the high optical transmission (over 60%) in the wavelength region of 435–800 nm. The other feature is that it acts as an effective isoelectronic dopant and improves the molar ratio of copper to iodine, which greatly enhances the near-band-edge emissions (411 and 432 nm) and suppresses the broadband emission (680 nm). The decay time of the fast emission under pulsed X-ray excitation is shorter than 450 ps. The results will give a guidance for optimizing the properties of γ-CuI single crystal as an ultrafast scintillator.

1. Introduction

γ-CuI is a p-type semiconductor and has an ultrafast scintillation component with the decay time of 130 ps, which exhibits great superiority in high-time-resolution radiation measurements [1,2]. Meanwhile, it also has many particular features such as direct band gap up to 3.1 eV [3], exciton binding energy up to 62 meV [4], etc.

There exist three phase-transition temperatures below the melting point of CuI, the growth of γ-CuI from the melt is impossible [4]. Various routes have been explored to grow bulk γ-CuI single crystals, such as sublimation [5], hydrothermal [6,7] flux [8], sol-gel [9], oxygen-free temperature reduction [10,11] and evaporation [12]. For the size of the crystal, the flux, hydrothermal and oxygen-free methods have obtained the crystals near 1.5 cm. But the flux and hydrothermal methods need rigorous setups, and the yield ratio is very low, especially for the flux method that is easy to form an intermediate KCu_4I_5 phase [8]. The sizes of the crystals grown through the sublimation and traditional evaporation are all less than 1 cm. Thus, it is still a great challenge to grow large-sized γ-CuI single crystals with excellent performance.

Evaporation in pure acetonitrile is deemed to be a suitable technique for fabrication of γ-CuI single crystals [13]. However, it has difficulty in obtaining the single crystal with its size larger than 1 cm because of the low solubility of CuI in pure acetonitrile. The increase in the concentration of I^- (iodide ions) can promote the dissolution of CuI in acetonitrile [11]. In our preliminary experiments, it has been found that LiI can promote the dissolution of CuI in acetonitrile. That is to say, the addition of LiI could be helpful for fabrication of larger γ-CuI single crystal in acetonitrile through evaporation technique.

The X-ray excited optical luminescence of γ-CuI single crystal consists of two components, which are the near-band-edge emission (ultrafast component with a decay time less than 1 ns) and a broadband emission near 680 nm (slow component), respectively [14]. Unfortunately, the intensity of the fast component is weak while that of the slow component is very strong [14]. Hence, the scintillation property of the single crystal should be improved through enhancing the intensity of the ultrafast component and suppressing that of the slow component. The nature of the broadband emission near 680 nm is ascribed to the deficiency of iodine [14]. It could form F center due to an electron trapped at a negative-ion vacancy, as the same as the deficiency of halide in many alkali halide single crystals [15]. Evidently, it is essential to increase the iodine content in the γ-CuI single crystal. The addition of iodine compound in γ-CuI single crystals during the crystal growth is a good approach to solve the problem. From the above analyses, it may be an effective route to grow larger γ-CuI single crystals with better scintillation performance by adding LiI in acetonitrile during the crystal growth.

In the present study, the solubility of γ-CuI with LiI in acetonitrile

* Corresponding author.
E-mail address: mgu@tongji.edu.cn (M. Gu).

https://doi.org/10.1016/j.materresbull.2018.06.010
Received 26 February 2018; Received in revised form 1 June 2018; Accepted 6 June 2018
Available online 07 June 2018
0025-5408/

was measured, and the concentration of LiI and evaporation technique for the crystal growth were optimized. As a result, a large-sized γ-CuI single crystal with good transparency was obtained. The properties of the single crystals were measured and discussed.

2. Experiment

2.1. Solubility study

In order to study the solubility variation of CuI caused by the addition of LiI in acetonitrile solvent, the solubility of CuI in different LiI concentration acetonitrile solvents was tested firstly. The starting materials involving CuI (99.5%) and acetonitrile (99.5%) were supplied from Sinopharm Chemical Reagent Co. Ltd. LiI (99.999%) was supplied from Alfa Aesar Co., Inc. All the starting materials were used without purification. It is reported that the lowest growth temperature which can successfully obtain γ-CuI single crystals is 45 °C [16]. On the other hand, the solubility of CuI in acetonitrile has negative temperature dependence [13]. In order to obtain large-sized γ-CuI single crystals, the initial growth temperature was 45 °C. The solubility of CuI in concentrations of 0.000, 0.001, 0.005, 0.010, 0.020, 0.030 and 0.040 mol/L LiI acetonitrile solvent was measured at 45 °C using weight loss analysis, the detailed experimental procedures were described in the reported paper [17].

Fig. 1(a) shows the solubility curve of CuI in acetonitrile with different concentration of LiI at 45 °C. It clearly illustrates that the addition of LiI can greatly increase the solubility of CuI in acetonitrile. The solubility is as high as 38.5 g/l in 0.040 mol/L LiI acetonitrile solvent.

The previous experiments show that high concentration of LiI leads γ-CuI to grow into polycrystalline shape with dark color. The proper concentration of LiI is about 0.005 mol/L. In order to understand the temperature dependence of the solubility with the addition of LiI and difference between it and that without the addition of LiI, the solubility of CuI in both 0.005 mol/L LiI acetonitrile and pure acetonitrile was measured at the temperature from 30 to 70 °C with an interval of 5 °C. Fig. 1(b) shows the results of both cases. The solubility of CuI in 0.005 mol/L LiI acetonitrile solvent can be expressed as

$$S = 44.61 - 0.44t,$$

where S is the solubility (g/L), and t is the temperature (°C). It indicates that the addition of LiI can greatly promote CuI to dissolve in acetonitrile with the temperature between 30–70 °C.

2.2. Crystal growth

The growth of bulk γ-CuI single crystals was scheduled in 0.005 mol/L LiI acetonitrile solvent at 45 °C. At first, the CuI and LiI powder were dissolved into acetonitrile solvent at 45 °C. The starting concentration of CuI was set as 22 g/L, which is lower than the saturation concentration of CuI in LiI acetonitrile at 45 °C. Then the 1000 ml beaker was filled with the 800 ml of the prepared solution which was filtered using the four-level filter papers. At last, the beaker was sealed with a single-deck plastic film before being transferred to the incubator. Fig. 1(a) has clearly illustrated that the solubility of CuI in acetonitrile solvent can be increased by a higher concentration of LiI. So with the evaporation of the solvent, the concentration of LiI is enhanced, thus increasing the solubility of CuI. As shown in Fig. 1(c), the solution is unsaturated at the early stage of the acetonitrile evaporation. With the acetonitrile evaporation, the solution begins to be saturated. After that, the saturation concentration of CuI increases with the decreasing in the volume of the acetonitrile solvent because of the increase of LiI concentration. This will slow down the growth rate of γ-CuI single crystals. So it is very important to improve the growth rate through designing temperature programming. The detailed temperature raising procedures were in the similar way reported in the literature [13]. Before the temperature increasing, the solution was maintained at 44 °C for three days to further reduce the number of crystal nucleus.

2.3. Characterization

The structure of obtained CuI crystal was detected by using an X-ray diffractometer (XRD, Haoyuan DX2700). The element contents of Li and Cu were measured by an inductively coupled plasma optical emission spectrometry (ICP-OES, PerkinElmer Optima 8000). The optical transmission of the crystal was measured using a JASCO V570 spectrometer. The photoluminescence (PL) spectra and the excitation spectra of the crystals were measured by using a fluorescence spectrophotometer (Edinburgh FLS920). The excitation source was a xenon lamp with the wavelength of 325 nm. The X-ray excited optical luminescence spectra of the crystals were conducted with an X-ray excited fluorescence spectrometer. The X-ray source was an F-30III X-ray tube with W anode target operating under 80 kV and 4 mA, and the spectrum detector was made with a Zolix SBP300 monochrometer and a Hamamatsu PMTH-S1-CR131 photomultiplier. The decay time curve of the 680 nm emission excited by 325 nm ultraviolet light was measured by the fluorescence spectrophotometer (Edinburgh FLS920) using a half-width of 1.0–1.6 ns hydrogen flashlamp as the excitation source. The decay time curves of fast luminescence of the crystal were performed by a streak camera. An ultrafast pulse laser (EKSPLA PL3140, 351 nm) with the pulse width of 10 ps was used as the excitation light source. The optical filters were used to block the scattered light and the test range is 1 ns. The decay time of the fast emission excited by X-ray was measured by a pulsed X-ray facility where the pulsed X-ray was generated by a half-width of 100 fs laser (532 nm, 10 TW, Amplitude Systemes) through a Cu target, and a microchannel plate photomultiplier tube (PMT140, Photex) was used to detect the emission of the crystal. The detector and crystal were placed in a closed container made of aluminum foil to prevent the interference of scattered excitation light. The transit time fluctuation of PMT140 is about 450 ps. All of

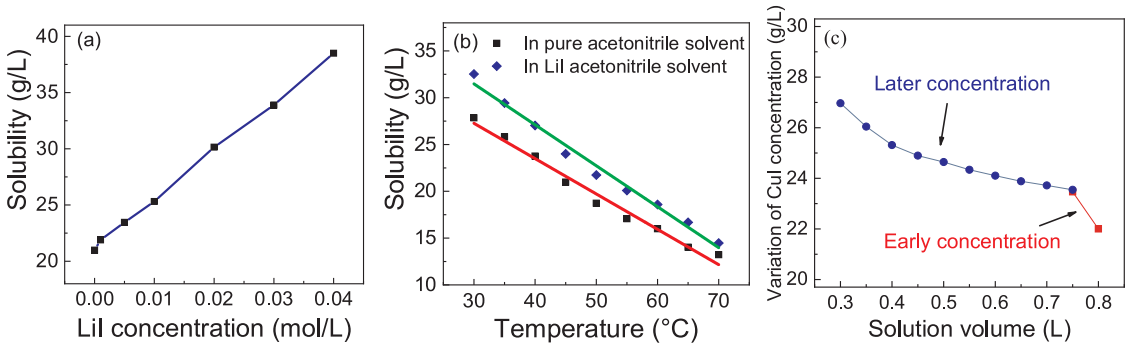

Fig. 1. (a) The solubility curve of CuI in LiI acetonitrile solvent as a function of LiI concentration at 45 °C; (b) the solubility curves of CuI in pure and 0.005 mol/L LiI acetonitrile solvents as a function of the temperature; (c) the solubility variation of CuI in LiI acetonitrile solvent with the evaporation of acetonitrile at 45 °C.

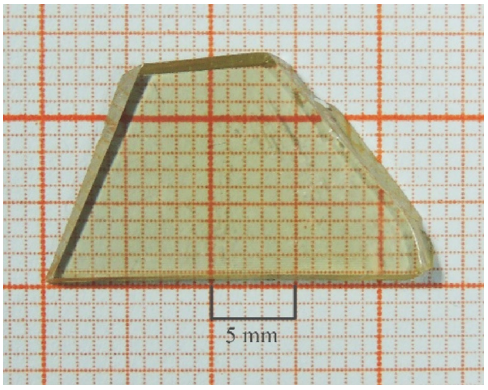

Fig. 2. photograph of the γ-CuI single crystal grown in LiI acetonitrile solvent.

the tests were conducted at room temperature.

3. Results and discussion

3.1. Crystal quality

The photograph of the CuI crystal grown in 0.005 mol/L LiI acetonitrile solvent is shown in Fig. 2. The crystal size is as large as 23 × 14 × 2 mm^3, which is larger than the crystal grown in pure acetonitrile solvent [13,16]. It clearly demonstrates that LiI is of great significance for the growth of large-sized CuI single crystals although the shape of the crystal has not been regular enough and requires further study.

3.2. Structural property and element analysis

Fig. 3 shows the XRD patterns of the CuI crystal grown in LiI acetonitrile solvent through evaporation technique and its pulverized crystals. It indicates that all of the diffraction peaks of the samples are matched well with those of γ-CuI (JCPDS card No. 06-0246). And the revealed crystal plane of γ-CuI grown in LiI acetonitrile solvent is the (111) crystal plane.

In order to confirm whether Li^+ (lithium-ion) is introduced into the

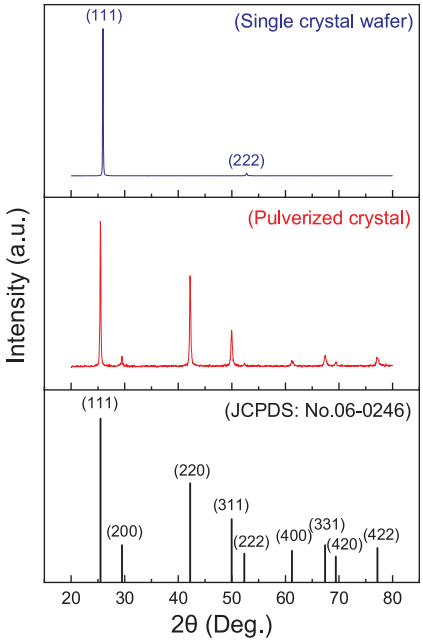

Fig. 3. XRD patterns of CuI single crystal wafer and pulverized crystal grown in LiI acetonitrile solvent, and JCPDS card.

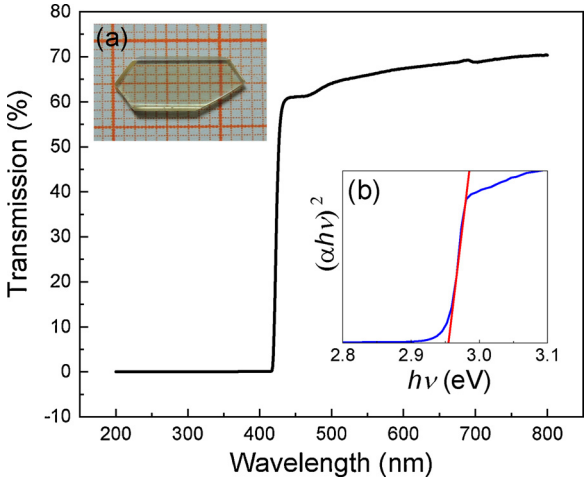

Fig. 4. Optical transmission of the γ-CuI single crystal grown in LiI acetonitrile solvent. The inset (a) is the fine polished γ-CuI single crystal, the inset (b) is the plot of $(ah\nu)^2$ vs $h\nu$.

γ-CuI single crystal, the element components were determined using an inductively coupled plasma optical emission spectrometry. The result reveals that the incorporation of Li^+ is 0.02 mol%, and the contents of Cu^+ and I^- are 48.92 mol% and 51.06 mol%, respectively, in γ-CuI single crystal. It shows that Li^+ is successfully introduced into γ-CuI single crystal and the content of I^- is improved by the addition of LiI, as compared to the crystal grown by traditional acetonitrile evaporation method, in which the contents of Cu^+ and I^- were 53.1% and 46.9%, respectively [18].

3.3. Optical transmittance

The crystal shown in the inset of Fig. 4 was cut and polished into a wafer with the thickness of 1.36 mm for the optical transmittance measurement. It is observed that the crystal has a transparent window over 60% in the visible region as shown in Fig. 4. The optical bandgap of the as-grown single crystal is determined by the property of the direct bandgap of the semiconductor. The graph of the variation of $(ah\nu)^2$ with $h\nu$ is given in the inset of Fig. 4. The bandgap is calculated to be 2.955 ± 0.001 eV, which is a little larger than that of the γ-CuI crystal grown without LiI [19]. The absorption spectra of samples grown with and without LiI are shown in Fig. 5. Both of them show intensive absorption at the edge of 415 nm, which is the characteristic of direct-gap interband transitions [7].

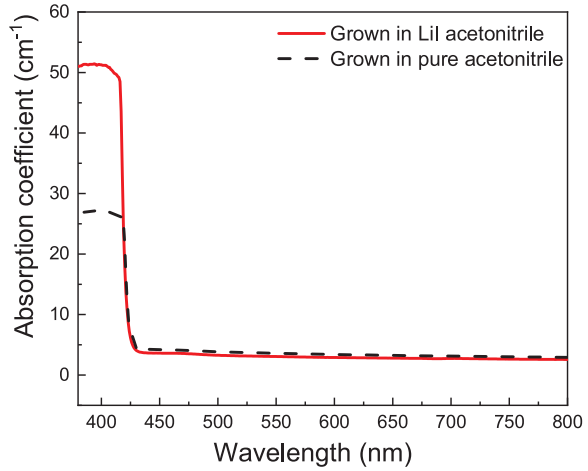

Fig. 5. Absorption spectra of the γ-CuI crystals grown in pure and LiI acetonitrile solvents.

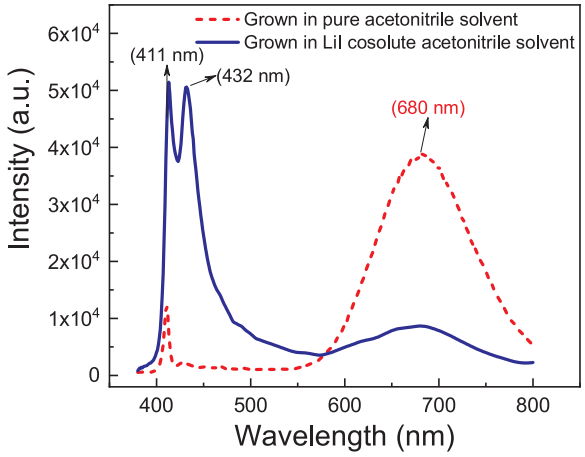

Fig. 6. PL of γ-CuI single crystals grown in pure and LiI acetonitrile solvents.

3.4. Photoluminescence

The PL spectra of the crystals grown with and without LiI are shown in Fig. 6. The crystal grown without LiI has two emission bands located at 411 nm and near 680 nm, respectively. The 411 nm emission originates from the free-exciton emission [20]. The 680 nm emission is related to the deficiency of iodine [14]. The PL spectrum of the crystal grown with LiI is quite different from that grown without LiI. The free-exciton emission (411 nm) has been enhanced. Meanwhile, the 680 nm emission is suppressed, which demonstrates that the deficiency of iodine in γ-CuI single crystal is reduced greatly as is been verified by ICP-OES. Additionally, an emission peak at 432 nm is observed in the crystal grown with LiI. It is well known that if a semiconductor was doped with isoelectronic impurities with different electronegativity, the more electropositive (or electronegative) impurity can trap holes (or electrons) [21]. In this work, the electronegativity of Li^+ is 0.98 which is quite lower than that of Cu^+ (1.90), and Li^+ could act as a hole trap when it substitutes Cu^+ in the crystal [21,22]. The 432 nm emission could be related to the recombination of electrons to isoelectronic hole traps on the Li_{Cu}. The excitation spectra monitoring the three peaks are shown in Fig. 7. There are no obvious excitation peaks for 411 and 432 nm emissions. While the excitation peak for 680 nm is located at 415 nm.

3.5. X-ray excited optical luminescence

The X-ray excited optical luminescence spectra of the crystals grown with and without LiI are exhibited in Fig. 8. Both crystals have a near-band-edge emission at 430 nm and a broadband near 680 nm. Although the whole intensity of luminescence is enhanced, the ratio of the intensity of 430 nm emission to that of 680 nm emission is obviously improved by the addition of LiI. The enhancement of near-band-edge emission could be the result of the additional recombination of electrons to isoelectronic hole traps on the Li_{Cu}, and the increase of 680 nm emission is likely due to the fact that its excitation peak is at the near-band-edge emission band and the transmittance of the crystal is improved. In order to know the relative scintillation efficiency of the crystal, a $PbWO_4$ single crystal with the same size was tested for comparison. The X-ray excited optical luminescence spectra of the samples are shown in Fig. 9. It can be calculated that the light yield of ultrafast emission for the γ-CuI single crystal is about 40% of that for $PbWO_4$.

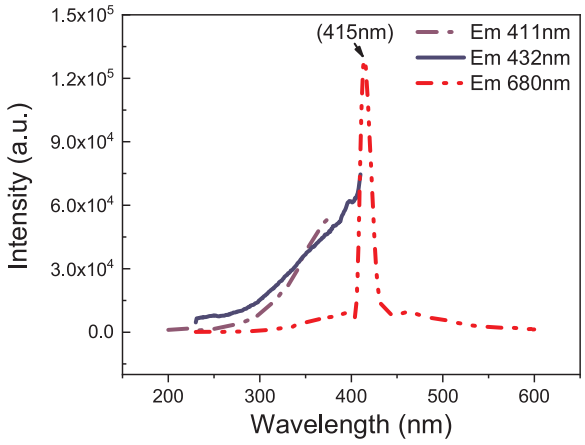

Fig. 7. The excitation spectra of the γ-CuI single crystal grown in LiI acetonitrile solvent.

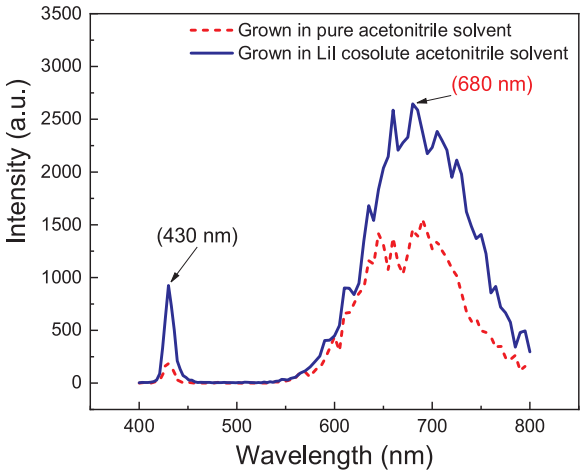

Fig. 8. X-ray excited optical luminescence spectra of γ-CuI single crystals grown in pure and LiI acetonitrile solvents.

3.6. Decay time

Fig. 10 depicts the decay curves of the emissions at 411, 432 and 680 nm of the crystal grown with LiI. The decay times of 411 and 432 nm emissions are 26.5 and 24.5 ps, respectively. They illustrate that both emissions belong to ultrafast luminescence. For the 680 nm emission, the luminescence intensity $I(t)$ can be expanded by two exponential decay components [23],

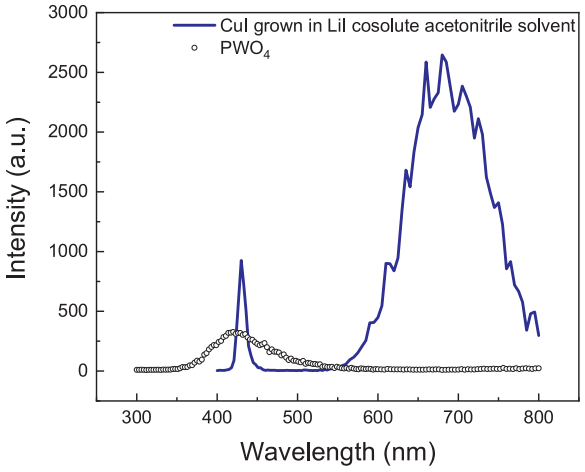

Fig. 9. The X-ray excited optical luminescence of γ-CuI and $PbWO_4$ single crystals.

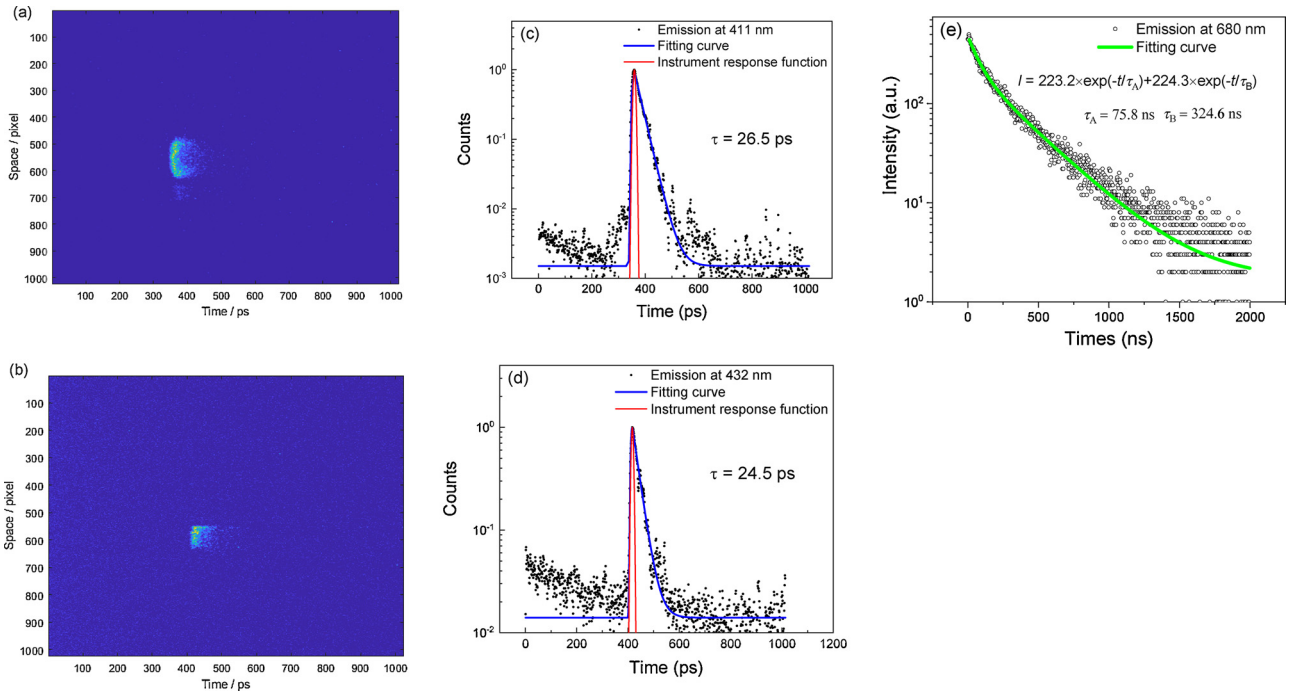

Fig. 10. The streak images of the emission at 411 nm (a) and 432 nm (b), the decay curves of the emission at 411 nm (c), 432 nm (d) and 680 nm (e) for the γ-CuI single crystal grown in LiI acetonitrile solvent.

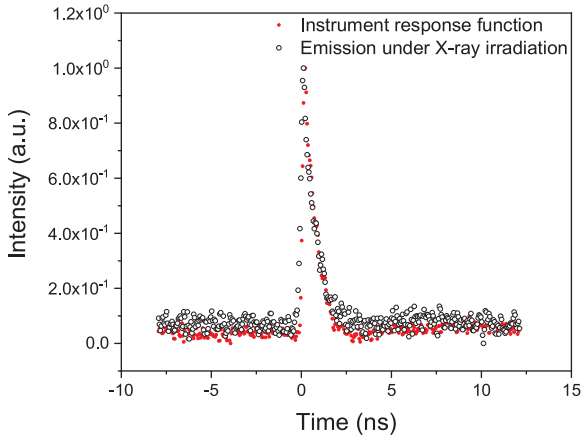

Fig. 11. The decay curve of the fast emission for the γ-CuI single crystal under pulsed X-ray excitation.

$$I(t) = A_1 \times \exp(-t/\tau_1) + A_2 \times \exp(-t/\tau_2), \quad (1)$$

where τ_1 and τ_2 represent the decay times of short- and long-decay components, respectively, parameters A_1 and A_2 are weight factors. The average decay time is determined by,

$$\langle\tau\rangle = \frac{(A_1\tau_1^2 + A_2\tau_2^2)}{(A_1\tau_1 + A_2\tau_2)} \quad (2)$$

The average decay time of 680 nm emission is 224 ± 7 ns, which includes two components, i.e., 76 ± 5 ns (18.86%) and 325 ± 6 ns (81.14%).

The 411 nm free exciton emission has ultrafast decay time because of the oscillator strength enhancement [24]. With regard to the decay time of the 432 nm emission, it could be understood that Li^+ can trap the exciton, as discussed above, and this trapped exciton emission usually has ultrafast decay time [21]. The same phenomenon was also reported in ZnO:Ga [25].

The decay time of the fast emission of the γ-CuI single crystal under pulsed X-ray excitation measured with fluorescence spectrophotometer is shown in Fig. 11. The decay curve is overlapped with the response function of the pulsed X-ray facility. It illustrates that the decay time of the fast emission is less than that of the detection limit (450 ps), i.e. less than 450 ps.

4. Conclusion

γ-CuI single crystals with transmittance over 60% in visible region were grown in LiI acetonitrile solvent through evaporation technique. The single crystal with the dimension of 23 × 14 × 2 mm^3 is the largest at present, and it has an excellent crystallinity. The addition of LiI in the crystal growth can greatly enhance the near-band-edge emissions (411 and 432 nm) and suppress the broadband emission (680 nm) of the crystal, respectively, because Li can act as an effective isoelectronic dopant and the addition of LiI can improve the molar ratio of copper to iodine. The decay times of the 411, 432 and 680 nm emissions under ultraviolet excitation are 26.5 ps, 24.5 ps, and 224 ns, respectively. Due to the limitation of the instrumentation used, it can only know that the fast decay time under X-ray excitation is less than 450 ps. The growth method by addition of LiI may provide an instruction for the optimum of the γ-CuI single crystal as an ultrafast scintillator.

Acknowledgment

The work is funded by the Significant National Special Project of the Ministry of Science and Technology of China for Development of Scientific Instruments and Equipment (Grant No. 2011YQ13001902) and the National Natural Science Foundation of China (Grant Nos. 11475128, 11675121 and 11775160).

References

[1] S.E. Derenzo, M.J. Weber, M.K. Klintenberg, Nucl. Instrum. Methods Phys. Res. Sect. A 486 (2002) 214–219.
[2] S.Q. Yue, M. Gu, X.L. Liu, F.R. Li, J.N. Zhang, S.M. Huang, B. Liu, C. Ni, Mater. Res. Bull. 101 (2018) 210–214.
[3] S. Lewonczuk, J. Ringeissen, E. Beaurepaire, M.A. Khan, Phys. Rev. B: Condens. Matter Mater. Phys. 49 (1994) 2344–2350.
[4] M. Grundmann, F.-L. Schein, M. Lorenz, T. Böntgen, J. Lenzner, H. von Wenckstern,

Phys. Status Solidi A 210 (2013) 1671–1703.
[5] T. Goto, T. Takahashi, M. Ueta, J. Phys. Soc. Jpn. 24 (1968) 314–327.
[6] V.A. Nikitenov, V.I. Popolitov, S.G. Stoyukhin, A.Y. Shapiro, A.N. Lobachev, A.I. Tereshchenko, V.G. Kolotilova, Sov. Technol. Phys. Lett. 5 (1979) 493–495.
[7] D.G. Chen, Y.J. Wang, Z. Lin, J.K. Huang, X.Z. Chen, D.M. Pan, F. Huang, Cryst. Growth Des. 10 (2010) 2057–2060.
[8] C. Schwab, A. Goltzene, Prog. Cryst. Growth Charact. 5 (1982) 233–276.
[9] M. Gu, D.X. Wang, Y.T. Huang, R. Zhang, Cryst. Res. Technol. 39 (2004) 1104–1107.
[10] B.Q. Lou, J.F. Zhang, H. Luo, J.G. Pan, J.G. Pan, J. Cryst. Growth. 388 (2014) 1–4.
[11] Y.Y. Lv, Z.H. Xu, L.W. Ye, Z.J. Zhang, G.B. Su, X.X. Zhuang, Crystengcomm. 17 (2015) 862–867.
[12] M. Gu, P. Gao, X.L. Liu, S.M. Huang, B. Liu, C. Ni, R.K. Xu, J.M. Ning, Mater. Res. Bull. 45 (2010) 636–639.
[13] P. Gao, M. Gu, X. Liu, C.F. Yang, Y.Q. Zheng, E.W. Shi, Crystengcomm. 15 (2013) 2934–2938.
[14] P. Gao, M. Gu, X.L. Liu, B. Liu, S.M. Huang, Appl. Phys. Lett. 95 (2009) 221904.
[15] R.K. Swank, F.C. Brown, Phys. Rev. 130 (1963) 34–41.
[16] J.G. Pan, S.Y. Yang, Y.B. Li, L. Han, X. Li, Y.J. Cui, Cryst. Growth Des. 9 (2009) 3825–3827.
[17] S.Q. Yue, M. Gu, X.L. Liu, J.N. Zhang, S.M. Huang, B. Liu, C. Ni, Opt. Mater. 66 (2017) 308–313.
[18] Z.X. Cai, M. Gu, X.L. Liu, B. Liu, S.M. Huang, C. Ni, Spectrosc. Spect. Anal. 33 (2013) 293–296.
[19] P. Gao, M. Gu, X. Liu, Y.Q. Zheng, E.W. Shi, Cryst. Res. Technol. 47 (2012) 707–712.
[20] D. Kim, M. Nakayama, O. Kojima, I. Tanaka, H. Ichida, T. Nakanishi, H. Nishimura, Phys. Rev. B. 60 (1999) 13879–13884.
[21] S.E. Derenzo, E. Bourret-Courshesne, G. Bizarri, A. Canning, Nucl. Instrum. Methods Phys. Res. Sect. A. 805 (2016) 36–40.
[22] T.C. Madden, J.L. Merz, G.L. Miller, D.G. Thomas, IEEE Trans. Nucl. Sci. 15 (1968) 47–57.
[23] S. Saha, S. Das, U.K. Ghorai, N. Mazumder, B.K. Gupta, K.K. Chattopadhyay, Dalton Trans. 42 (2013) 12965–12974.
[24] J. Wilkinson, K.B. Ucer, R.T. Williams, Radiat. Meas. 38 (2004) 501–505.
[25] E.D. Bourret-Courchesne, S.E. Derenzo, M.J. Weber, Nucl. Instrum. Methods Phys. Res. Sect. A 601 (2009) 358–363.